

ENTRANCE-CHANNEL EFFECTS IN THE DYNAMICAL CLUSTER-DECAY MODEL FOR THE DECAY OF HOT AND ROTATING COMPOUND NUCLEUS $^{48}\text{Cr}^*$ AT $E_{CN}^* \approx 60$ MeV

BIRBIKRAM SINGH*, MANOJ K. SHARMA*,
RAJ K. GUPTA^{†,‡,§} and WALTER GREINER[‡]

* *Thapar Institute of Engineering and Technology (Deemed University),
Patiala-147004, India*

[†] *Department of Physics, Panjab University, Chandigarh-160014, India*

[‡] *Frankfurt Institute for Advanced Studies (FIAS),
Johann Wolfgang Goethe-Universität,*

Max-von-Laue-Str. 1, D-60438 Frankfurt am Main, Germany

Received 11 January 2006

The entrance-channel effects in the decay of hot and rotating compound nucleus $^{48}\text{Cr}^*$, formed in symmetric $^{24}\text{Mg} + ^{24}\text{Mg}$ and asymmetric $^{36}\text{Ar} + ^{12}\text{C}$ reactions, are studied as collective clusterization process, for emissions of both the light particles (LPs) as well as the intermediate mass fragments (IMFs), with in the dynamical cluster-decay model (DCM). We find that the little differences observed in the decay of equilibrated compound nucleus $^{48}\text{Cr}^*$, formed in the two entrance channels with about the same excitation energy, are *not* in variance with the Bohr's independence hypothesis. In other words, the present study confirms the entrance-channel independence of the decay of compound nucleus $^{48}\text{Cr}^*$ formed due to different target-projectile combinations with similar excitation energies. The collective clusterization process is shown to contain the complete structure of the measured fragment cross sections as well as average total kinetic energies.

Keywords: Dynamic cluster-decay model; entrance channels; hot and rotating compound nucleus.

1. Introduction

The compound nucleus $^{48}\text{Cr}^*$ is produced in a symmetric $^{24}\text{Mg} + ^{24}\text{Mg}$ ¹ as well as very asymmetric $^{36}\text{Ar} + ^{12}\text{C}$ reaction,² using different center-of-mass energies ($E_{c.m.} = 44.4$ and 47.0 MeV, respectively), such that the excitation energy E_{CN}^* ($= 59.4$ and 59.5 MeV, respectively) is nearly the same. This nucleus offers as an ideal example for studying the entrance-channel effects, since it belongs to the well established mass region $40 \leq A_{CN} \leq 80$ of fusion-fission phenomenon, and has also the observed data showing additional non-statistical reaction mechanisms, like the resonances, deep-inelastic or orbiting processes associated with such effects.^{3,4}

[§]DFG Mercator Guest Professor.

According to the independence hypothesis of Bohr,⁵ the excitation process leaves the compound nucleus (formed with fixed angular momentum and excitation energy) in a sufficiently complex state that the subsequent decay is statistical and independent of the formation process. The statistical model analysis in terms of the transition-state model (TSM),⁶ applied to the above mentioned data, shows^{1,2} that the mass and kinetic energy distributions are better reproduced for the symmetric-channel $^{24}\text{Mg}+^{24}\text{Mg}$ than that for the asymmetric-channel $^{36}\text{Ar}+^{12}\text{C}$. For the asymmetric channel, the calculated mass asymmetry is lower than that of the data, possibly due to the non-statistical processes. The entrance-channel effects are also found to be present in heavy compound systems ($A_{CN} \sim 160$),⁷⁻¹⁰ which are understood in terms of the increased fusion/formation times for more symmetric channels due to the added nuclear dissipative effects in the calculations.^{11,12}

In this paper, we study for the first time the entrance channel effects in the decay of $^{48}\text{Cr}^*$, formed via the symmetric and very asymmetric entrance channels, using the dynamical cluster-decay model (DCM) of Gupta and collaborator.¹³⁻¹⁹ Another interest of this study is the extension of the application of DCM to the decay of a further lighter compound nucleus; the lightest compound system studied so far on DCM is $^{56}\text{Ni}^*$. Like $^{56}\text{Ni}^*$, ^{48}Cr is also a negative Q-value (Q_{out}) system and would decay only if it is produced in heavy ion reactions with enough compound nucleus excitation energy, such that

$$E_{CN}^* - |Q_{\text{out}}(T)| = TKE(T) + TXE(T). \quad (1)$$

Here $E_{CN}^* = E_{c.m.} + Q_{in}$ and, $TXE(T)$ and $TKE(T)$ are the total excitation energy and total kinetic energy of the decay fragments, respectively. The Q-value of the entrance (incoming) channel $Q_{in} = 15.0$ and 12.5 MeV, respectively, for $^{24}\text{Mg}+^{24}\text{Mg}$ and $^{36}\text{Ar}+^{12}\text{C}$ reactions. The temperature $T=3.43$ MeV for the two reactions, obtained by using the expression

$$E_{CN}^* = (A_{CN}/9)T^2 - T. \quad (2)$$

The decay products considered are both the light particles (LPs) of mass ≤ 4 and the intermediate mass fragments (IMFs) constituting the remaining mass spectra. Experimental data for both the symmetric ($^{24}\text{Mg}+^{24}\text{Mg}$) and asymmetric ($^{36}\text{Ar}+^{12}\text{C}$) reactions are available for both the LPs and IMFs mass yields and average TKE.^{1,2}

The dynamical cluster-decay model (DCM) of preformed clusters for hot and rotating compound systems is presented in the Sec. 2 and its application to the decay of compound nucleus $^{48}\text{Cr}^*$ formed in $^{24}\text{Mg}+^{24}\text{Mg}$ and $^{36}\text{Ar}+^{12}\text{C}$ reactions is presented in Sec. 3. The idea of the calculations is to look for the entrance-channel effects, if any. Our results are summarized in the Sec. 4.

2. The Dynamical Cluster-Decay Model (DCM)

In DCM, the decay of hot and rotating compound nucleus is studied as the dynamical collective clusterization process for both the LPs and IMFs emissions. This

is in contrast to the statistical models^{6,20,21,22} where the two types of emissions are treated differently; the LPs as the evaporation and IMFs as fission processes. Moreover, the missing structure information of the compound system in statistical models enters the DCM via the preformation probabilities of the fragments.

The DCM is worked out in terms of the collective coordinates of mass asymmetry $\eta = \frac{A_1 - A_2}{A_1 + A_2}$ and relative separation R , which allow to define the decay cross-section, in terms of the partial waves, as

$$\sigma = \frac{\pi}{k^2} \sum_{\ell=0}^{\ell_c} (2\ell + 1) P_0 P; \quad k = \sqrt{\frac{2\mu E_{c.m.}}{\hbar^2}}, \quad (3)$$

where the preformation probability P_0 refers to η motion and the penetrability P to R motion. Apparently, the two motions are taken as decoupled, an assumption justified in the earlier works.^{23,24,25} The critical angular momentum,

$$l_c = R_a \sqrt{2\mu[E_{c.m.} - V(R_a, \eta_{in}, l=0)]}/\hbar, \quad (4)$$

with $\mu(= \frac{A_1 A_2}{A_1 + A_2} m)$ as the reduced mass and m the nucleon mass.

For η -motion, we solve the stationary Schrödinger equation in η , at a fixed R ,

$$\left\{ -\frac{\hbar^2}{2\sqrt{B_{\eta\eta}}} \frac{\partial}{\partial \eta} \frac{1}{\sqrt{B_{\eta\eta}}} \frac{\partial}{\partial \eta} + V_R(\eta, T) \right\} \psi_R^{(\nu)}(\eta) = E_R^{(\nu)} \psi_R^{(\nu)}(\eta), \quad (5)$$

with $\nu = 0, 1, 2, 3, \dots$ and $R = R_a = C_t(\eta, T) + \overline{\Delta R}(T)$, an ansatz, first used in (13) for the first turning point and for the decay of a hot compound nucleus. For $T = 0$, $\overline{\Delta R}(T) = 0$. The C_i , in $C_t = C_1 + C_2$, are the Süßmann central radii $C_i = R_i(T) - b^2/R_i(T)$ with $R_i(T) = r_0(T)A_i^{1/3} = 1.07(1 + 0.01T)A_i^{1/3}$ and the surface thickness parameter $b(T) = 0.99(1 - 0.99T^2)$ fm. The eigen solutions of Eq. (5) give the preformation probability at a given temperature T , as

$$P_0(A_i) = |\psi_R(\eta)|^2 \sqrt{B_{\eta\eta}} \frac{2}{A} = \sum_{\nu=0}^{\infty} |\psi_R^{(\nu)}|^2 \exp(-E_R^{(\nu)}/T) \sqrt{B_{\eta\eta}} \frac{2}{A}. \quad (6)$$

The mass parameters $B_{\eta\eta}$, representing the kinetic energy part in Eq. (5), are the smooth classical hydro-dynamical masses,²⁶ since at the temperatures of interest here the shell effects are almost completely washed out.

The fragmentation potential $V_R(\eta, T)$ at any temperature T , in Eq. (5), is calculated within the Strutinsky renormalization procedure, as

$$V_R(\eta, T) = \sum_{i=1}^2 [V_{\text{LDM}}(A_i, Z_i, T)] + \sum_{i=1}^2 [\delta U_i] \exp(-T^2/T_0^2) + V_c(T) + V_P(T) + V_l(T), \quad (7)$$

where the T-dependent liquid drop energy $V_{\text{LDM}}(T)$ is that of Ref. 27, with (Seeger's) constants at $T = 0$ refitted to give the experimental binding energies

B ,²⁸ defined as $B = V_{\text{LDM}}(T = 0) + \delta U$. The shell corrections δU are calculated in the “empirical method” of Myers and Swiatecki,²⁹ which are considered to vanish exponentially for $T_0 = 1.5$ MeV.³⁰ The V_P is an additional attraction due to the nuclear proximity potential,³¹

$$V_P(R, T) = 4\pi\bar{R}(T)\gamma b(T)\phi(s, T), \quad (8)$$

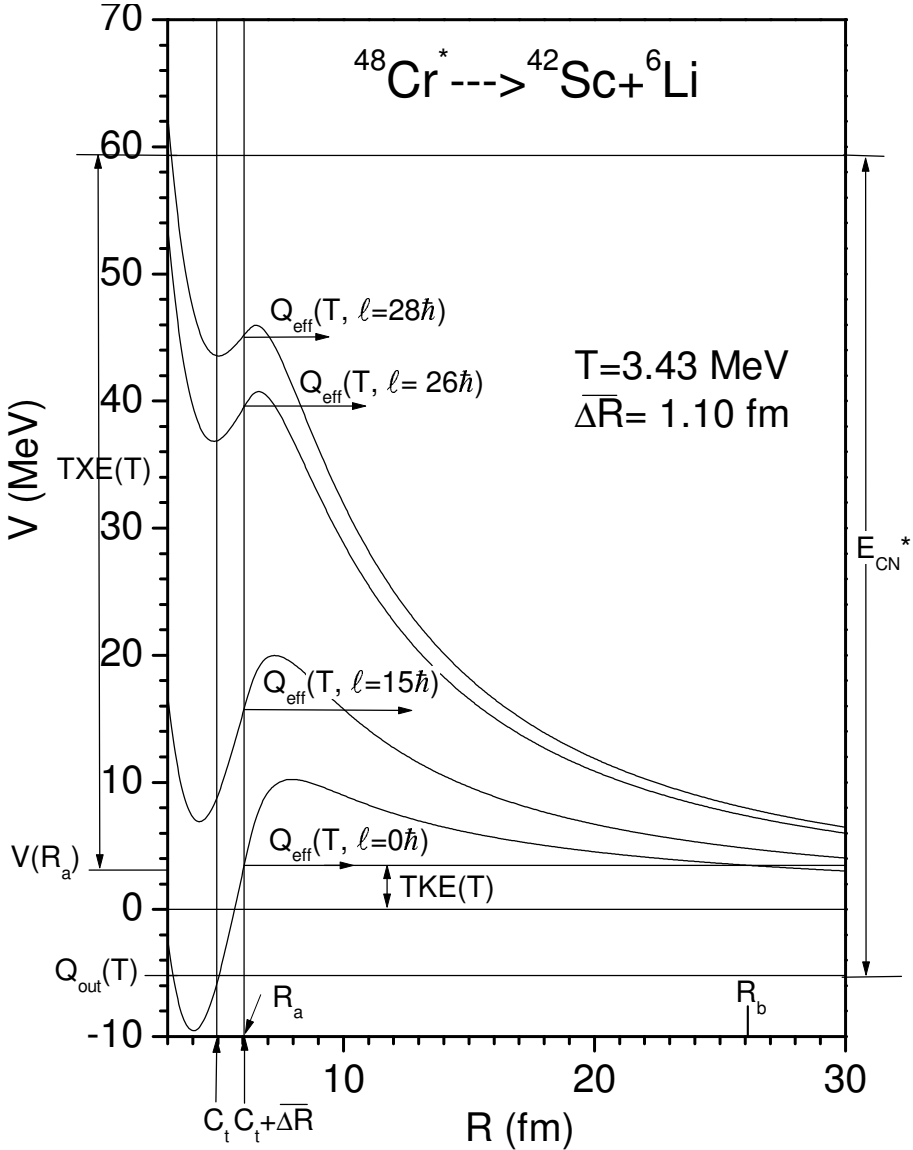


Fig. 1. The scattering potential for the decay $^{48}\text{Cr}^* \rightarrow ^{42}\text{Sc} + ^6\text{Li}$ at temperature $T = 3.43$ MeV and different l -values.

with γ , $\overline{R}(T)$ and $\phi(s, T)$, respectively, as the specific nuclear surface tension coefficient, the inverse of the root-mean-square radius of the Gaussian curvature and the universal function. The Coulomb potential $V_c = \frac{Z_1 Z_2 e^2}{R(T)}$, where the charges are fixed by minimizing the potential $V_R(\eta, T)$ in charge asymmetry coordinate $\eta_Z = \frac{Z_1 - Z_2}{Z_1 + Z_2}$. The angular momentum effects are calculated by equation

$$V_l(T) = \frac{\hbar^2 l(l+1)}{2I(T)} \quad (9)$$

with moment of inertia, in complete sticking limit (≤ 2 fm), given by $I(T) = I_S(T) = \mu R_a^2 + \frac{2}{5} A_1 m C_1^2 + \frac{2}{5} A_2 m C_2^2$.

The scattering potential $V(R, T)$, normalized to the exit-channel binding energy, is given as

$$V(R, T) = V_c(T) + V_P(T) + V_l(T), \quad (10)$$

with the potential $V(R = R_a)$, corresponding to first turning point, acting like an effective, positive Q-value, Q_{eff} , for the decay of the hot compound nucleus at T to two fragments in the exit-channel observed in ground states ($T = 0$). The Q_{eff} is independently defined, in terms of the respective binding energies $B(T)$, as

$$Q_{\text{eff}}(T) = B(T) - [B_1(T = 0) + B_2(T = 0)] = TKE(T) = V(R_a). \quad (11)$$

Since, at $T = 0$, $TKE(T = 0) = Q_{\text{out}}$ and $R_a = C_t(\eta)$, the $\Delta R(\eta)$ in $R = R_a = C_t(\eta, T) + \Delta R(\eta, T)$ corresponds to the change in TKE at T with respect to its value at $T = 0$, and hence can be estimated exactly for the temperature effects added in the scattering potential $V(R)$. Note that here ΔR is taken to be η -dependent, whereas the average $\overline{\Delta R}$ assimilates the effects of both the deformations and η dependences.

The tunneling probability P is calculated as the WKB penetrability,

$$P_i = \exp\left(-\frac{2}{\hbar} \int_{R_a}^{R_b} \{2\mu[V(R) - Q_{\text{eff}}]\}^{1/2} dR\right), \quad (12)$$

solved analytically,³² with the first and second turning points R_a and R_b satisfying $V(R_a) = V(R_b) = Q_{\text{eff}}$ (see Fig. 1). Finally, the l -dependence of R_a is defined by

$$V(R_a) = Q_{\text{eff}}(T, \ell = 0), \quad (13)$$

i.e. R_a is the same for all ℓ -values, given by the above equation, and that $V(R_a, \ell) = Q_{\text{eff}}(T, \ell)$. Then, using (13), $R_b(\ell)$ is given by the ℓ -dependent scattering potentials (10).

3. Calculations

The total or critical angular momentum of the compound system formed depends on the entrance-channel mass asymmetry η_{in} and the entrance-channel c.m. energy $E_{c.m.}$ [Eq. (4)], which are different for the symmetric and asymmetric entrance-channels so as to obtain nearly the same compound nucleus excitation energy E_{CN}^* .

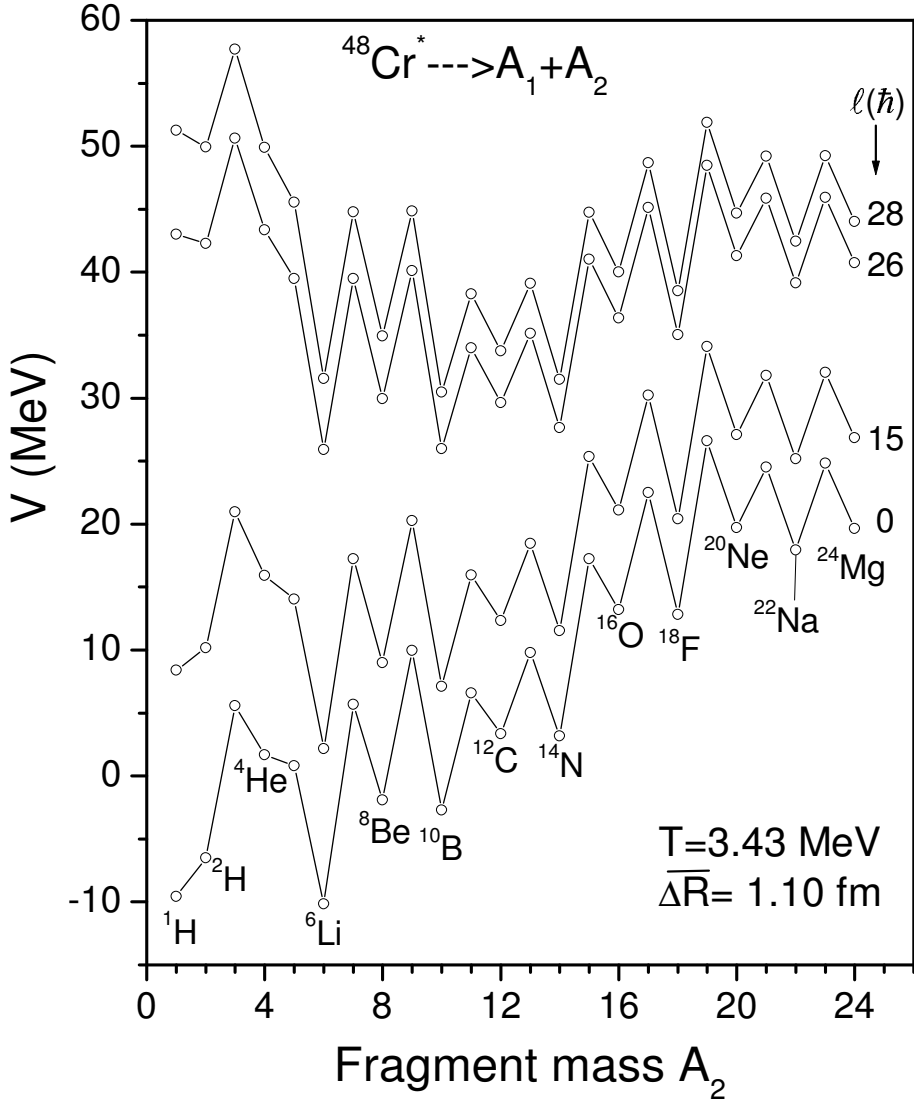


Fig. 2. Fragmentation potential for the decay of $^{48}\text{Cr}^*$ at $T = 3.43$ MeV, $R = C_t + \overline{\Delta R}$ ($\overline{\Delta R} = 1.10$ fm), and at different l -values.

For $^{48}\text{Cr}^*$ system, $l_c = 28$ and $26\hbar$, respectively, for the symmetric $^{24}\text{Mg}+^{24}\text{Mg}$ and asymmetric $^{36}\text{Ar}+^{12}\text{C}$ entrance-channels.

Figure 2 gives the calculated fragmentation potential for the decay of $^{48}\text{Cr}^*$ into various mass fragments (LPs and IMFs) at $T = 3.43$ MeV of the experimental data, and different l -values. We notice that the structure of the potential energy surface does not change much in going from $l = 26$ (the l_c -value for $^{24}\text{Mg}+^{24}\text{Mg}$) to $28\hbar$ (the l_c -value for $^{36}\text{Ar}+^{12}\text{C}$), even though the characteristic behaviour of

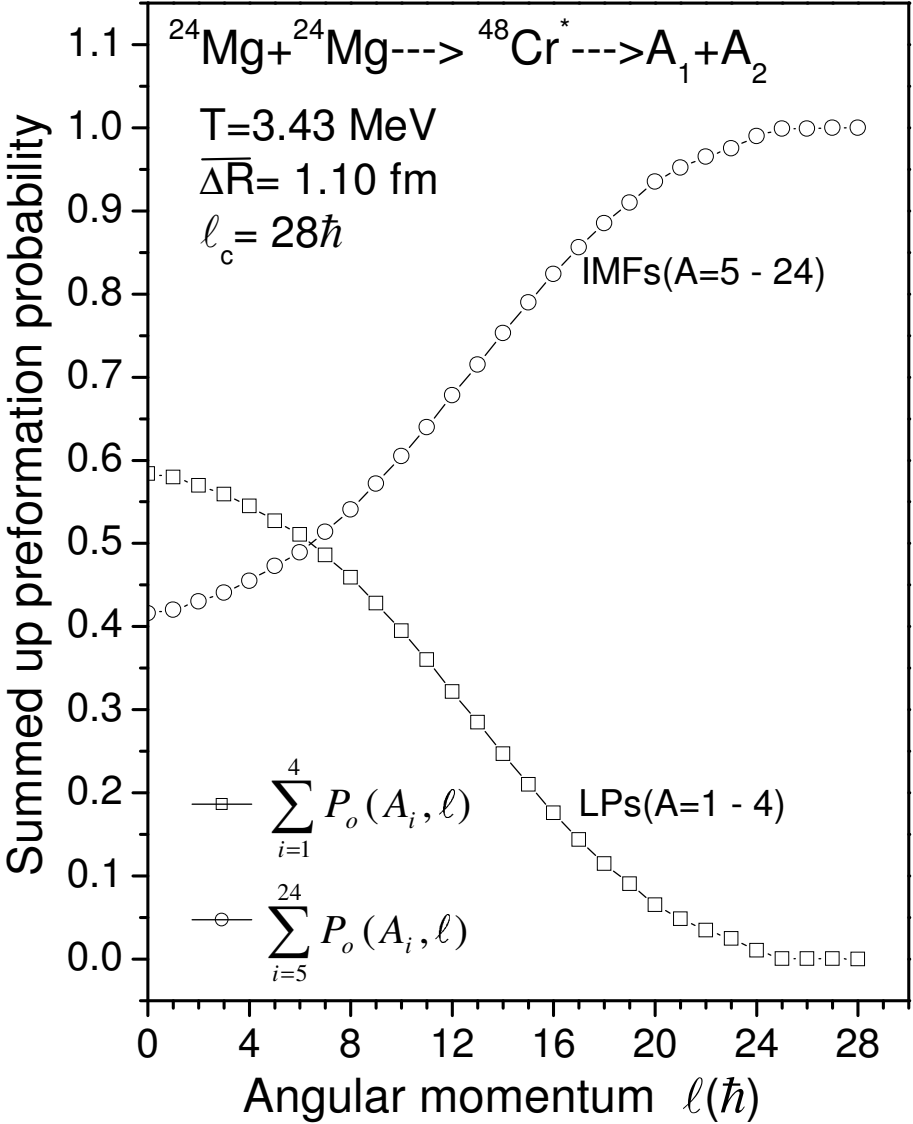


Fig. 3. The summed up preformation probability P_0 for the LPs and IMFs, shown as a function of $l(\hbar)$ for the decay of compound system $^{48}\text{Cr}^*$ formed in the symmetric $^{24}\text{Mg} + ^{24}\text{Mg}$ channel.

the fragmentation potential for LPs and IMFs are different at the lower versus higher l -values. At lower l -values, the LPs are energetically more favourable (lower in energy), whereas the same is true of IMFs at higher l -values. This result is further illustrated in Figs. 3 and 4, respectively, for the summed up preformation probability P_0 and penetration probability P , for the case of $l_c = 28\hbar$. The $\sum P_0$ is larger for LPs at lower l 's whereas it is larger for IMFs at higher l 's. The $\sum P$,

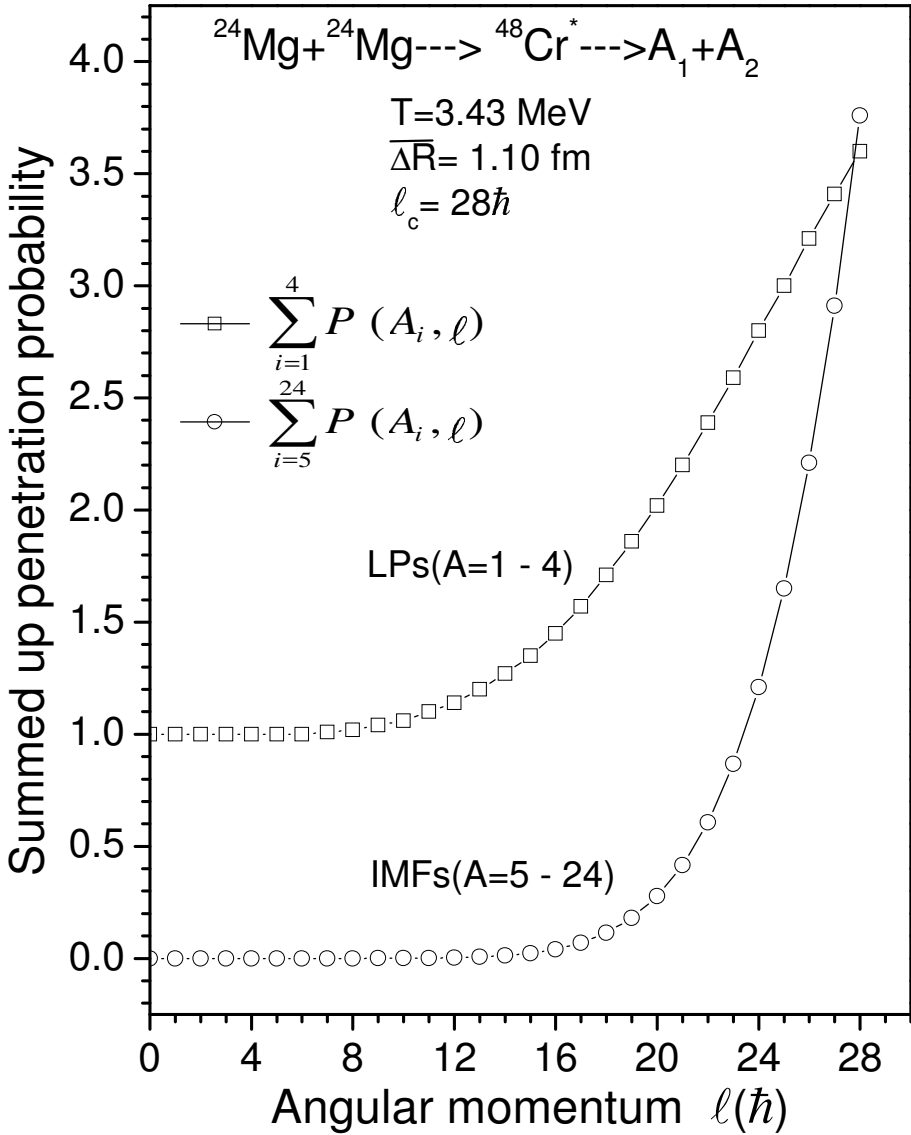


Fig. 4. Same as for Fig. 3, but for penetration probability P .

however, becomes larger for IMFs only for $l > 26\hbar$, the l_c -value for the symmetric-channel case.

The calculated P_0 as a function of fragment mass is shown in Fig. 5 for different l -values. Comparing Figs. 3 and 5, we notice that, though the summed up P_0 does not change much, its magnitude as a function of fragment mass shows a considerable change, for both the LPs and heavy mass fragments ($20 \leq A_2 \leq 24$), when l -value is changed by two units in the neighbourhood of l_c . However, these results

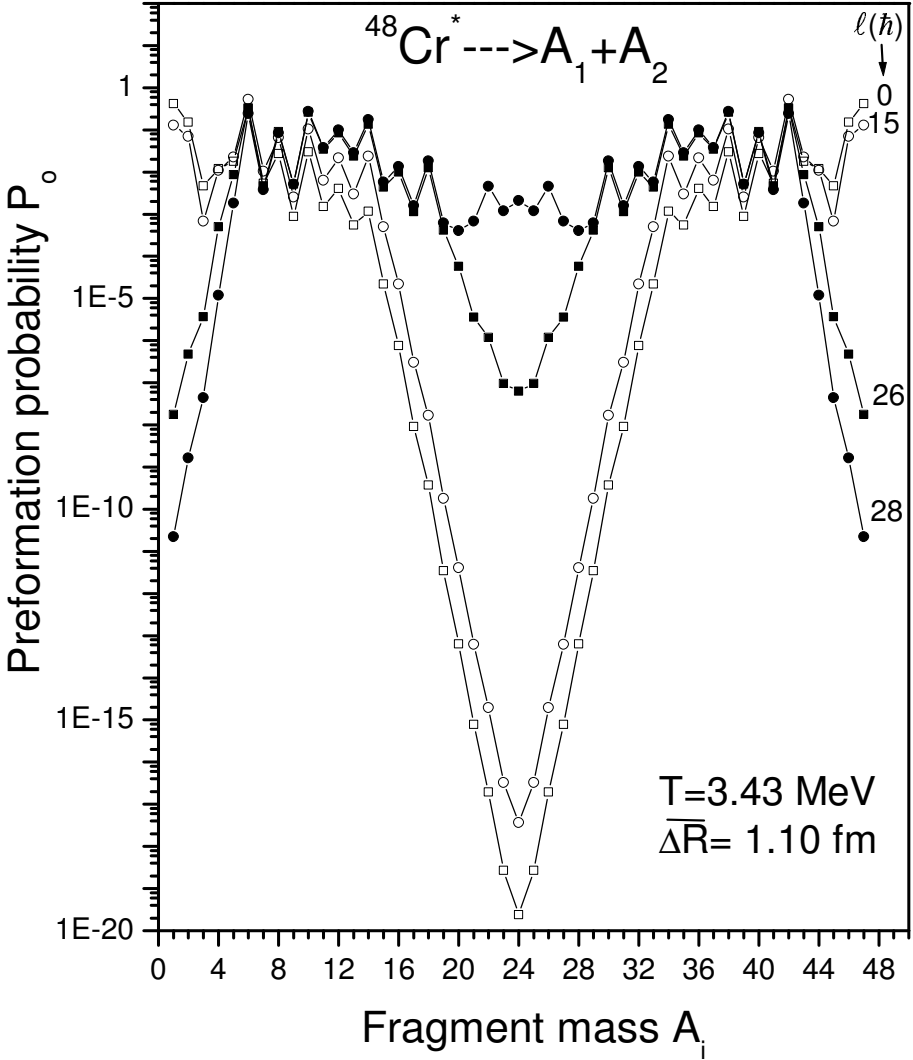


Fig. 5. Preformation probability P_0 as a function of fragment mass A_i for the decay of $^{48}\text{Cr}^*$, calculated by using the fragmentation potential of Fig. 2.

of the entrance-channel effects in P_0 are contrary to the behaviour presented by penetrability P in Fig. 6, i.e., the $P(A_2)$ does not change much by changing l_c by two units. In the following, we look for the consequences of these results for the cross-sections.

In Fig. 7, we have plotted the (decay) barrier heights $V_B(A_2, l)$ for $^{48}\text{Cr}^*$. We find that, in agreement with the earlier fission barrier calculations of Royer,³³ for low spins the V_B decreases, and hence the decay probability increases, with the increase of mass asymmetry (i.e. for LPs), whereas the same for higher spins increases with

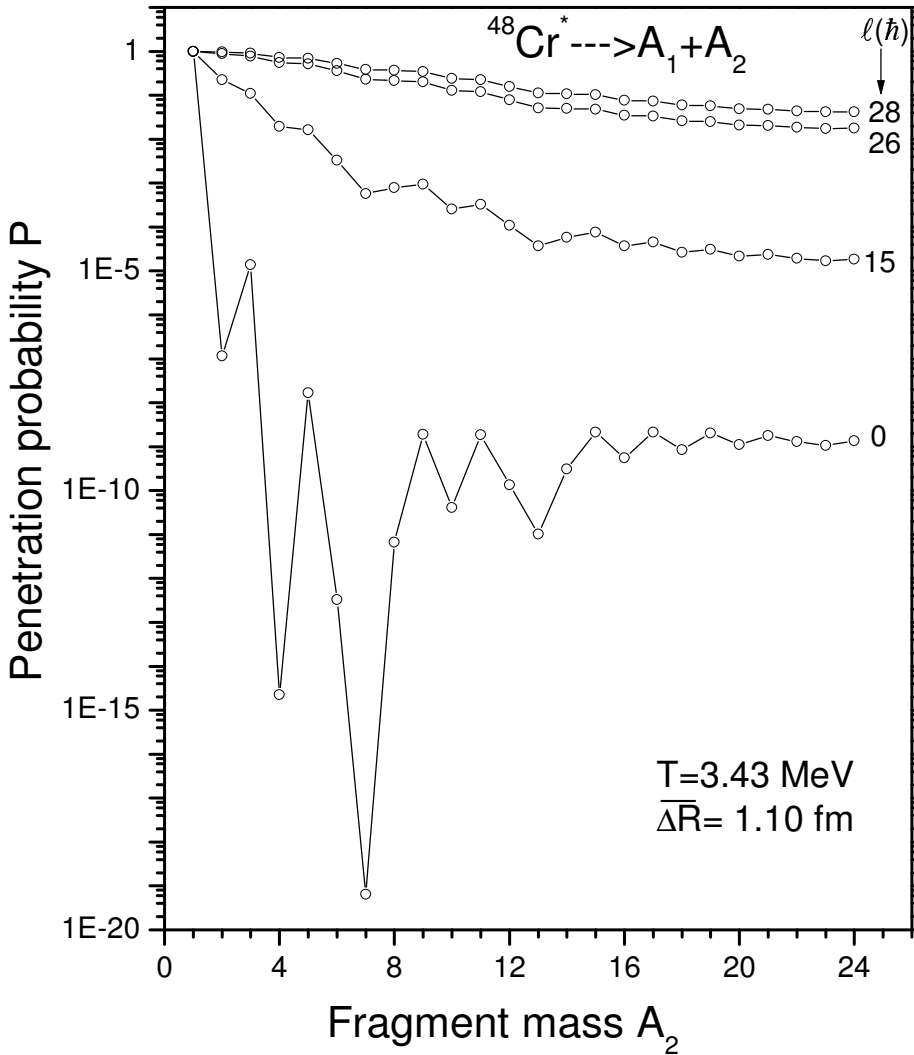


Fig. 6. Penetration probability P as a function of fragment mass A_2 for the decay of $^{48}\text{Cr}^*$.

the increase of mass asymmetry. Interestingly, this result remains the same for $l_c = 26$ and $28\hbar$, i.e. is independent of whether the compound nucleus $^{48}\text{Cr}^*$ is formed from symmetric $^{24}\text{Mg}+^{24}\text{Mg}$ or asymmetric $^{36}\text{Ar}+^{12}\text{C}$ channel.

Figure 8 shows the calculated cross-sections for the decay of compound nucleus $^{48}\text{Cr}^*$, formed via the two entrance-channels $^{24}\text{Mg}+^{24}\text{Mg}$ and $^{36}\text{Ar}+^{12}\text{C}$, into the LPs, the σ_{LP} (equivalently, σ_{evr} in the language of statistical model), and IMFs, σ_{IMF} , and their sum, the total cross-section σ_{Total} . The summed up cross-sections for $l = l_{\text{max}}$ are also shown here as a legend, where LPs = 1 – 4 and IMFs = 5 – 24. The following results are evident: (i) As expected, the lower l -values contribute only

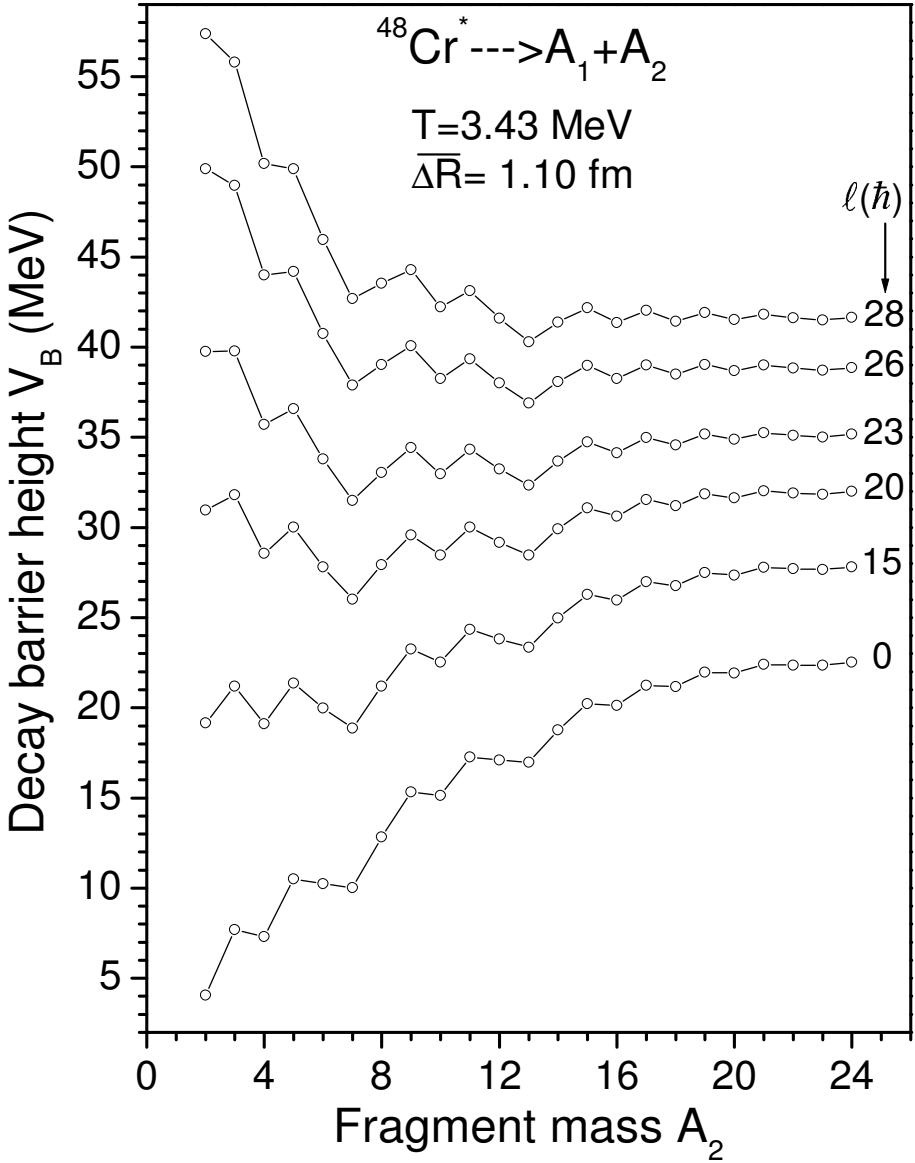


Fig. 7. The (decay) barrier heights for the decay of $^{48}\text{Cr}^*$ into various fragments (LPs and IMFs), calculated at different l -values.

towards σ_{LP} and at higher l -values the fission-like σ_{IMF} also starts to contribute. (ii) The σ_{LP} becomes zero at the *same* $l_{\max} = 25\hbar$ for the two entrance channels, a few units lower than the l_c -values. This result is a first clear signature of the independence of entrance-channel effects. In view of this result, we have presented our results in this figure up to l_{\max} only, and in the following also we sum up the angular momentum l -values up to l_{\max} , instead of l_c .

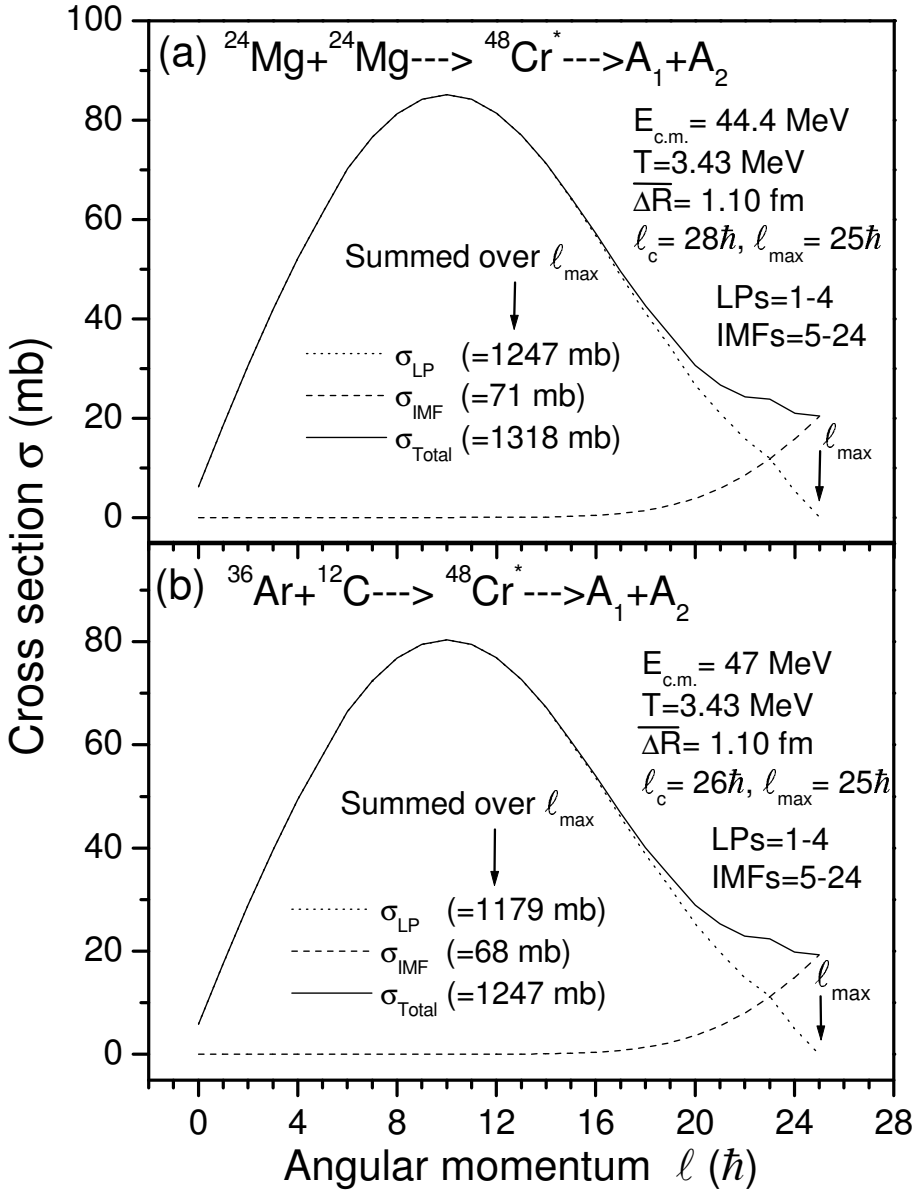


Fig. 8. Variation of the σ_{LP} , the σ_{IMF} and their sum σ_{Total} as a function to l for the decay of compound system $^{48}\text{Cr}^*$ formed in (a) symmetric and (b) asymmetric entrance channels. Here, LPs = 1 – 4 and IMFs = 5 – 24, in both the cases.

Table 1 shows the l_{max} -summed up results of our calculated σ_{LP} , σ_{IMF} and σ_{Total} , compared with the experimental data^{1,2} and the transition-state model (TSM) calculations^{1,2} for the two entrance-channels. Here, we take for LPs, the $A_2 = 1 - 4$ (as above), and for IMFs, as observed in experiments, $A_2 = 6 - 24$

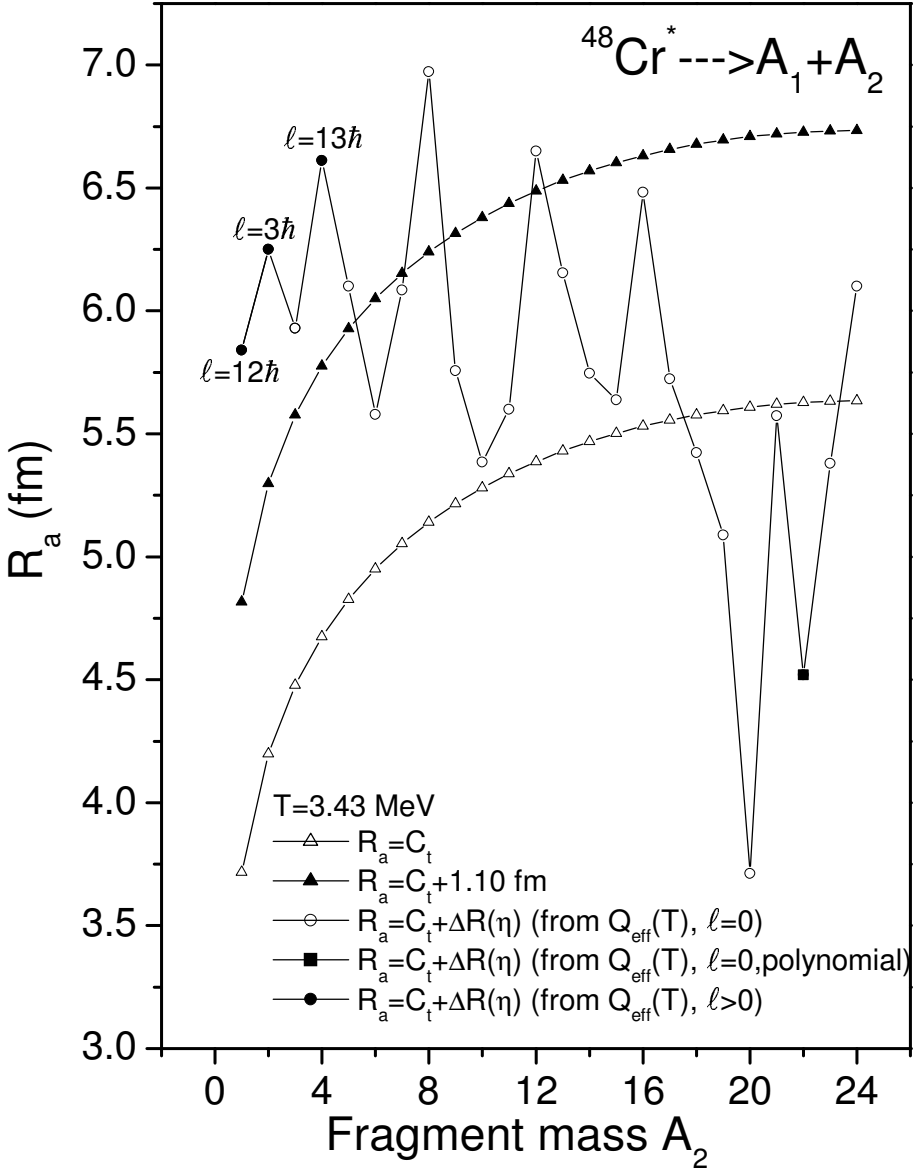


Fig. 9. Variation of the first turning point R_a with light fragment mass A_2 for fixed $\overline{\Delta R}=0$ and 1.10 fm, and one determined from Q_{eff} at $l=0$, or $l > 0$ (as mentioned in each case), or via a polynomial joining the minimum in $V(R)$ to $Q_{\text{out}}(T)$ for $l=0$ case.

and their complementary heavy fragments. For asymmetric-channel $^{36}\text{Ar} + ^{12}\text{C}$, the $A_2 = 8$ is not observed and hence is not included here too. Also presented in Table 1 are the results of another calculation where $R_a(\eta)$ or $\Delta R(\eta)$ are calculated from Q_{eff} (see Fig. 9 for $R_a(A_2)$). We find in Table 1 that the fits for DCM are of the

Table 1. The decay cross-sections for LPs ($A_2 = 1-4$), IMFs (as observed in experiments, i.e., $A_2 = 6-24$ and their complimentary heavy fragments, excluding $A_2 = 8$ in case of asymmetric-channel) and the Total, calculated on DCM for $\overline{\Delta R} = 1.10$ and $\Delta R(\eta)$ (in fm) for $l_{\max} = 25h$ and compared with TSM calculations and experiment data.^{1,2}

Reaction	$\sigma_{LP}(mb)$				$\sigma_{IMF}(mb)$				$\sigma_{Total}(mb)$			
	DCM $\overline{\Delta R}$	$\Delta R(\eta)$	TSM	Expt.	DCM $\overline{\Delta R}$	$\Delta R(\eta)$	TSM	Expt.	DCM $\overline{\Delta R}$	$\Delta R(\eta)$	TSM	Expt.
$^{24}\text{Mg}+^{24}\text{Mg}$	1247	789	1100	1065 ± 65	135	46	132^\dagger	150	1382	835	1232	1215 ± 65
$^{36}\text{Ar}+^{12}\text{C}$	1179	746	970	1215 ± 67	119	12	30	$25^{\dagger\dagger}$	1298	758	1000	1240 ± 67

[†]This number is stated to be 112 mb in Ref. 1, but from their Fig. 6, we get it as 132 mb.

^{††} Determined from Fig. 4 of Ref. 2.

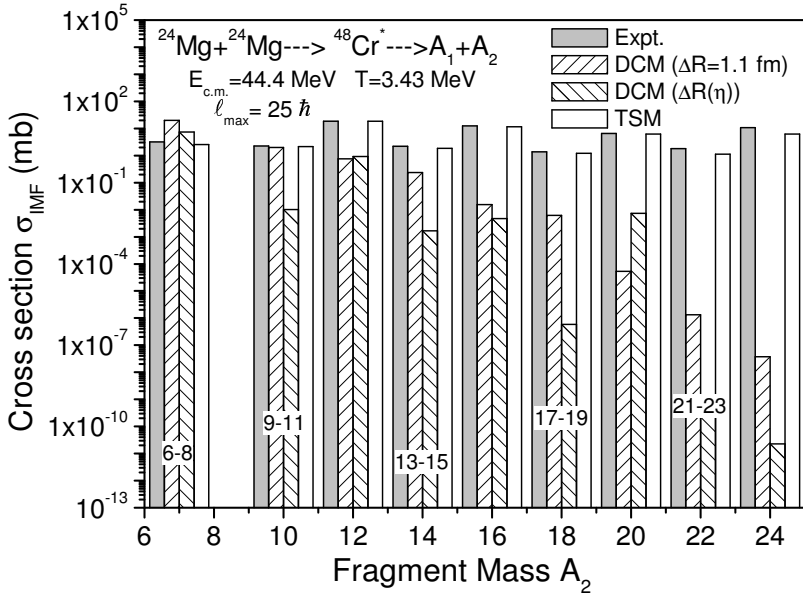


Fig. 10. The calculated σ_{IMF} on DCM for decay fragments of $^{48}\text{Cr}^*$ formed in symmetric entrance-channel $^{24}\text{Mg} + ^{24}\text{Mg}$, compared with the TSM and experimental data.

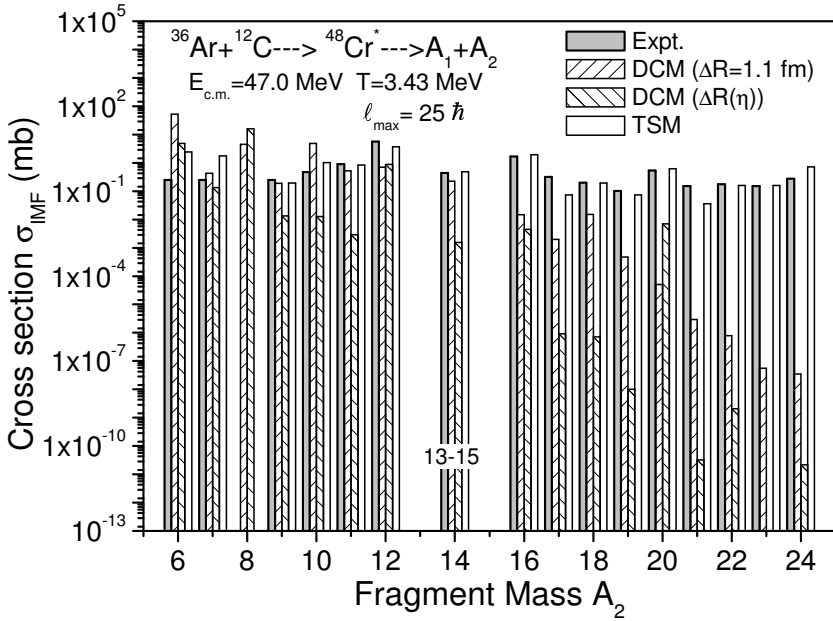


Fig. 11. The same as for Fig. 10, but for asymmetric entrance-channel $^{36}\text{Ar} + ^{12}\text{C}$.

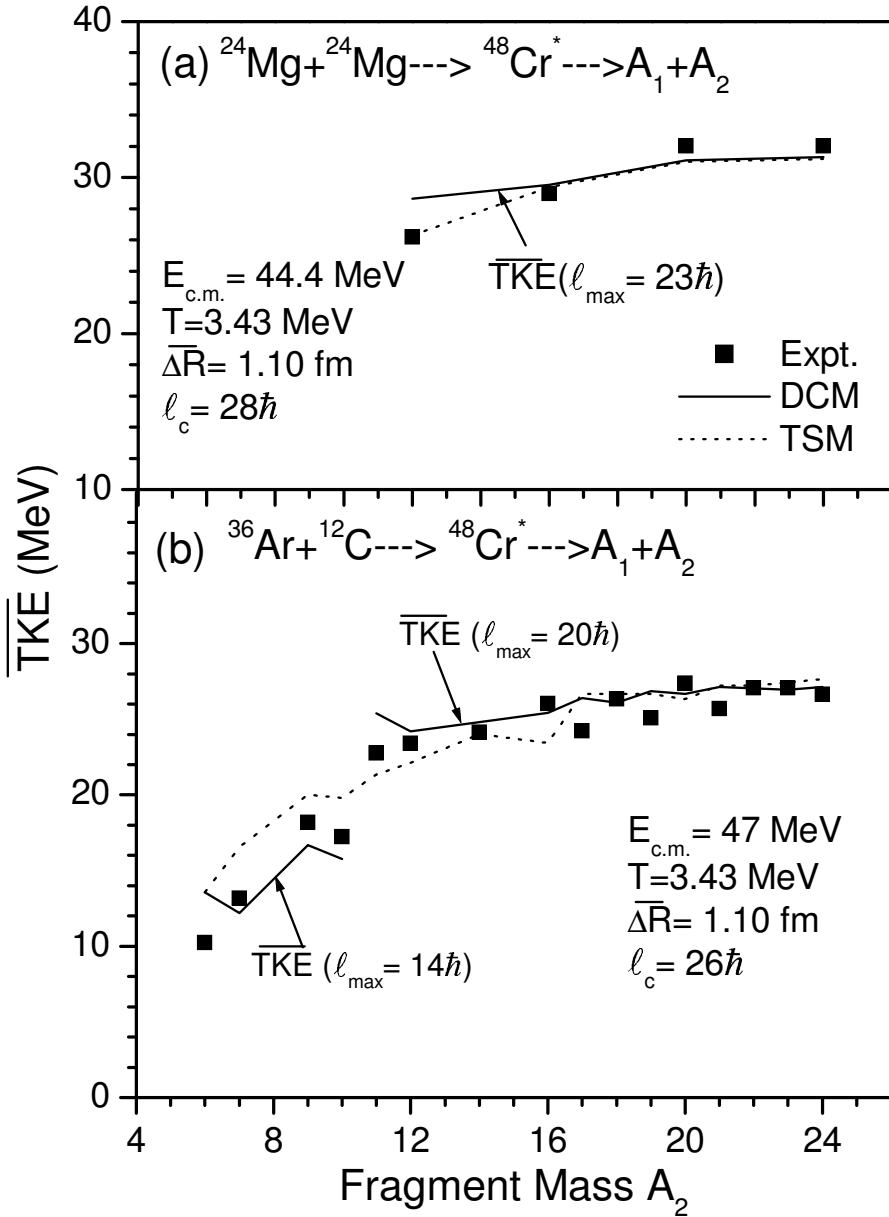


Fig. 12. The average total kinetic energy \overline{TKE} , calculated on DCM and compared with the TSM and experimental data, for the decay of compound system $^{48}\text{Cr}^*$ formed in (a) symmetric $^{24}\text{Mg} + ^{24}\text{Mg}$ and (b) asymmetric $^{36}\text{Ar} + ^{12}\text{C}$ entrance-channel.

same quality as for TSM, and it is nearly difficult to choose between the $\overline{\Delta R}$ and $\Delta R(\eta)$ results for DCM, though the constant $\overline{\Delta R}$ seems to work better on the whole. Another important result that follows from Table 1 is that the differences

in the numbers for all the three cross-sections due to the two entrance-channels are very small, and are of the same order as in experiments. Note that the large differences in the case of IMFs are due the fact that different fragments are observed in the two reactions. In other words, we find a reasonably good entrance-channel independence for the decay of $^{48}\text{Cr}^*$ formed in asymmetric or symmetric reactions.

As a further check on the DCM predictions, we have plotted in Figs. 10 and 11, the mass spectrum for IMFs, for the two entrance channels $^{24}\text{Mg}+^{24}\text{Mg}$ and $^{36}\text{Ar}+^{12}\text{C}$, respectively, compared with the TSM and experimental data.^{1,2} The data is grouped in the same way, as in experiments, and the average values plotted. Since the DCM does not include the non-compound nucleus effects, as expected,¹⁹ its results are good only for light fragments ($Z < 9$). Also, no effects of secondary light-particle emission are included in DCM, though these effects are known to be small² and are included in TSM calculations. In Fig. 11, ^8Be is also included for DCM though it was not accessible in experiments. Considering all these points and the comparisons in Table 1, the DCM predictions could be termed as in reasonably good agreement with the data. Since ^{12}C yield is observed to be maximum in both the reactions, we have also attempted to fit this yield via $\overline{\Delta R}$, the only parameter in DCM. We get an improved fit for $\overline{\Delta R} = 1.30$ fm, but then the other cross-sections get over-estimated.

Finally, the calculated average TKE,

$$\overline{TKE}(A_2) = \sum_{l=0}^{l_{\max}} \frac{\sigma_l(A_2)}{\sigma(A_2)} TKE(l, A_2);$$

with $\sigma = \sum_l \sigma_l$, is compared with the experimental data and TSM results^{1,2} in Fig. 12 for both the entrance channels. Apparently, our fits are as good as for TSM, but for $l_{\max} < l_c$ -values, and for the asymmetric-channel for two different l_{\max} -values. However, this has always been the case for DCM predictions of average \overline{TKE} ,¹⁸ not evident why.

4. Summary and Discussion of Results

The entrance channel effects are studied and the dynamical cluster-decay model (DCM) applied for the first time to the decay of a light compound nucleus $^{48}\text{Cr}^*$ formed in symmetric $^{24}\text{Mg}+^{24}\text{Mg}$ and asymmetric $^{36}\text{Ar}+^{12}\text{C}$ reactions, at incident energies $E_{c.m.} = 44.4$ and 47.0 MeV, respectively, but with same excitation energy $E_{CN}^* \approx 60$ MeV. The emission of both the LPs and IMFs is treated on the same footing. Though some of the characteristic quantities of the model do show entrance channel effects, the calculated cross-sections are found to be entrance-channel independent for the decay of the compound nucleus $^{48}\text{Cr}^*$. The calculated decay cross-sections for different fragments (the LPs and IMFs) are found to contain the complete structure of the experimental data and are in reasonably good agreement with it, particularly for the IMFs of mass $A \leq 20$. The calculated average kinetic energies (\overline{TKE} s) are also comparable with experimentally measured average TKEs.

Of course, it would be of further interest to study the effects of varying the excitation energy (equivalently, temperature) of the compound nucleus $^{48}\text{Cr}^*$, and the entrance-channel effects for the heavier compound systems.

Acknowledgments

One of the authors (MKS) is thankful to the Department of Science and Technology (DST), for support of this research work in the form of a Young Scientist's award under the SERC Fast Track Scheme. Another author (RKG) thanks the Deutsche-Forschungs-gemeinschaft (DFG), Germany, for the award of Mercator Guest Professorship.

References

1. A. T. Hasan, S. J. Sanders, K. A. Farrar, F. W. Prosser, B. B. Back, R. R. Betts, M. Freer, D. J. Henderson, R. V. F. Janssens, A. H. Wuosmaa and A. Szanto de Toledo, *Phys. Rev. C* **49** (1994) 1031.
2. K. A. Farrar, S. J. Sanders, A. K. Dummer, A. T. Hasan, F. W. Prosser, B. B. Back, I. G. Bearden, R. R. Betts, M. P. Carpenter, B. Crowell, M. Freer, D. J. Henderson, R. V. F. Janssens, T. L. Khoo, T. Lauritsen, Y. Liang, D. Nisius, A. H. Wuosmaa, C. Beck, R. M. Freeman, Sl. Cavallaro and A. Szanto de Toledo, *Phys. Rev. C* **54** (1996) 1249.
3. A. H. Wuosmaa, R. W. Zurmühle, P. H. Kutt, S. F. Pate, S. Saini, M. L. Halbert and D. C. Hensley, *Phys. Rev. C* **41** (1990) 2666.
4. S. P. Barrow, R. W. Zurmühle, D. R. Benton, Y. Miao, Q. Li, P. H. Kutt, Z. Liu, C. Lee, N. G. Wimer and J. T. Murgatroyd, *Phys. Rev. C* **52** (1995) 3088.
5. N. Bohr, *Nature (London)* **137** (1936) 344.
6. S. J. Sanders, *Phys. Rev. C* **44** (1991) 2676.
7. A. Ruckelshausen, R. D. Fischer, W. Kühn, V. Metag, R. Mühlhans, R. Novotny, T. L. Khoo, R. V. F. Janssens, H. Gröger, D. Habs, H. W. Heyng, R. Repnow, D. Schwalm, G. Duchêne, R. M. Freeman, B. Haas, F. Haas, S. Hlavac and R. S. Simon, *Phys. Rev. Lett.* **56** (1986) 2356.
8. B. Fornal, F. Gramegna, G. Prete, G. D'Erasmus, E. M. Fiore, L. Fiore, A. Pantaleo, V. Paticchio, G. Viesti, P. Blasi, F. Lucarelli, M. Anghinolfi, P. Corvisiero, M. Taiuti, A. Zucchiatti, P. F. Bortignon, Ch. Ferrer, G. Nardelli and G. Nebbia, *Phys. Rev. C* **42** (1990) 1472.
9. S. Flibotte, H. R. Andrews, T. E. Drake, A. Galindo-Uribarri, B. Haas, V. P. Janzen, D. Prévost, D. C. Radford, J. Rodriguez, P. Romain, J. P. Vivien, J. C. Waddington, D. Ward and G. Zwartz, *Phys. Rev. C* **45** (1992) R889.
10. P. Twin, *Nucl. Phys. A* **574** (1994) 51c.
11. M. Thoennessen and J. R. Beene, *Nucl. Phys. A* **557** (1993) 247c.
12. M. Thoennessen, E. Ramakrishnan, J. R. Beene, F. E. Bertrand, M. L. Halbert, D. J. Horen, P. E. Mueller and R. L. Varner, *Phys. Rev. C* **51** (1995) 3148.
13. R. K. Gupta, M. Balasubramaniam, C. Mazzocchi, M. La Commara and W. Scheid, *Phys. Rev. C* **65** (2002) 024601.
14. R. K. Gupta, R. Kumar, N. K. Dhiman, M. Balasubramaniam, W. Scheid and C. Beck, *Phys. Rev. C* **68** (2003) 014610.
15. M. Balasubramaniam, R. Kumar, R. K. Gupta, C. Beck and W. Scheid, *J. Phys. G: Nucl. Part. Phys.* **29** (2003) 2703.

16. R. K. Gupta, Acta Phys. Hung. (N.S.) *Heavy Ion Phys.* **18** (2003) 347.
17. R. K. Gupta, M. Balasubramaniam, R. Kumar, D. Singh and C. Beck, *Nucl. Phys. A* **738** (2004) 479c.
18. R. K. Gupta, M. Balasubramaniam, R. Kumar, D. Singh, C. Beck and W. Greiner, *Phys. Rev. C* **71** (2005) 014601.
19. R. K. Gupta, M. Balasubramaniam, R. Kumar, D. Singh, S. K. Arun and W. Greiner, *J. Phys. G: Nucl. Part. Phys.* (2005) submitted.
20. S. J. Sanders, D. G. Kovar, B. B. Back, C. Beck, D. J. Henderson, R. V. F. Janssens, T. F. Wang and B. D. Wilkins, *Phys. Rev. C* **40** (1989) 2091.
21. S. J. Sanders, A. T. Hasan, F. W. Prosser, B. B. Back, R. R. Betts, M. P. Carpenter, D. J. Henderson, R. V. F. Janssens, T. L. Khoo, E. F. Moore, P. R. Wilt, F. L. H. Wolfs, A. H. Wuosmaa, K. B. Beard and Ph. Benet, *Phys. Rev. C* **49** (1994) 1016.
22. J. Gomez del Campo, R. L. Auble, J. R. Beene, M. L. Halbert, H. J. Kim, A. D'Onofrio and J. L. Charvet, *Phys. Rev. C* **43** (1991) 2689.
23. J. Maruhn and W. Greiner, *Phys. Rev. Lett.* **32** (1974) 548.
24. R. K. Gupta, W. Scheid and W. Greiner, *Phys. Rev. Lett.* **35** (1975) 353.
25. D. R. Saroha and R. K. Gupta, *J. Phys. G* **12** (1986) 1265.
26. H. Kröger and W. Scheid, *J. Phys. G* **6** (1980) L85.
27. N. J. Davidson, S. S. Hsiao, J. Markram, H. G. Miller and Y. Tsang, *Nucl. Phys. A* **570** (1994) 61c.
28. G. Audi and A. H. Wapstra, *Nucl. Phys. A* **595** (1995) 4.
29. W. Myers and W. J. Swiatecki, *Nucl. Phys. A* **81** (1966) 1.
30. A. S. Jensen and J. Damgaard, *Nucl. Phys. A* **203** (1973) 578.
31. J. Blocki, J. Randrup, W. J. Swiatecki and C. F. Tsang, *Ann. Phys. (NY)* **105** (1977) 427.
32. S. S. Malik and R. K. Gupta, *Phys. Rev. C* **39** (1989) 1992; S. Kumar and R. K. Gupta, *Phys. Rev. C* **49** (1994) 1922.
33. G. Royer, *J. Phys. G: Nucl. Part. Phys.* **21** (1995) 249.